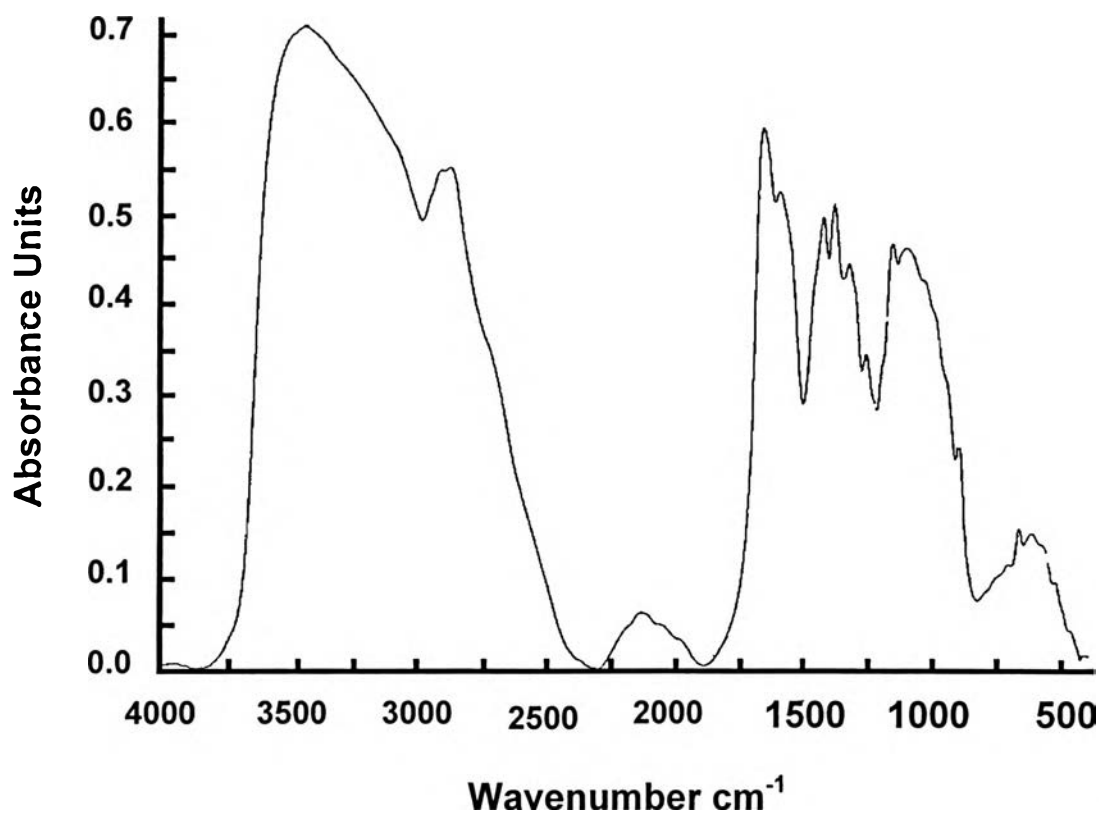# CHAPTER IV
RESULTS AND DISCUSSION

4.1 Chemical Structure Analysis of Chitosan

Owing to the limited amount of chitosan starting material used in the present work, two different degree of deacetylation chitosans were used, i.e., 85.9 and 75.8 %

FT-IR spectra of the chitosan starting materials are shown in Figure 4.1 and Figure 4.2.

Figure 4.1 FT-IR spectrum of chitosan (DD = 85.9 %).

FT-IR (KBr, cm^{-1}) :- 3417 (O-H), 2880 (C-H), 1657(C=O amide),1077(pyranose rings).
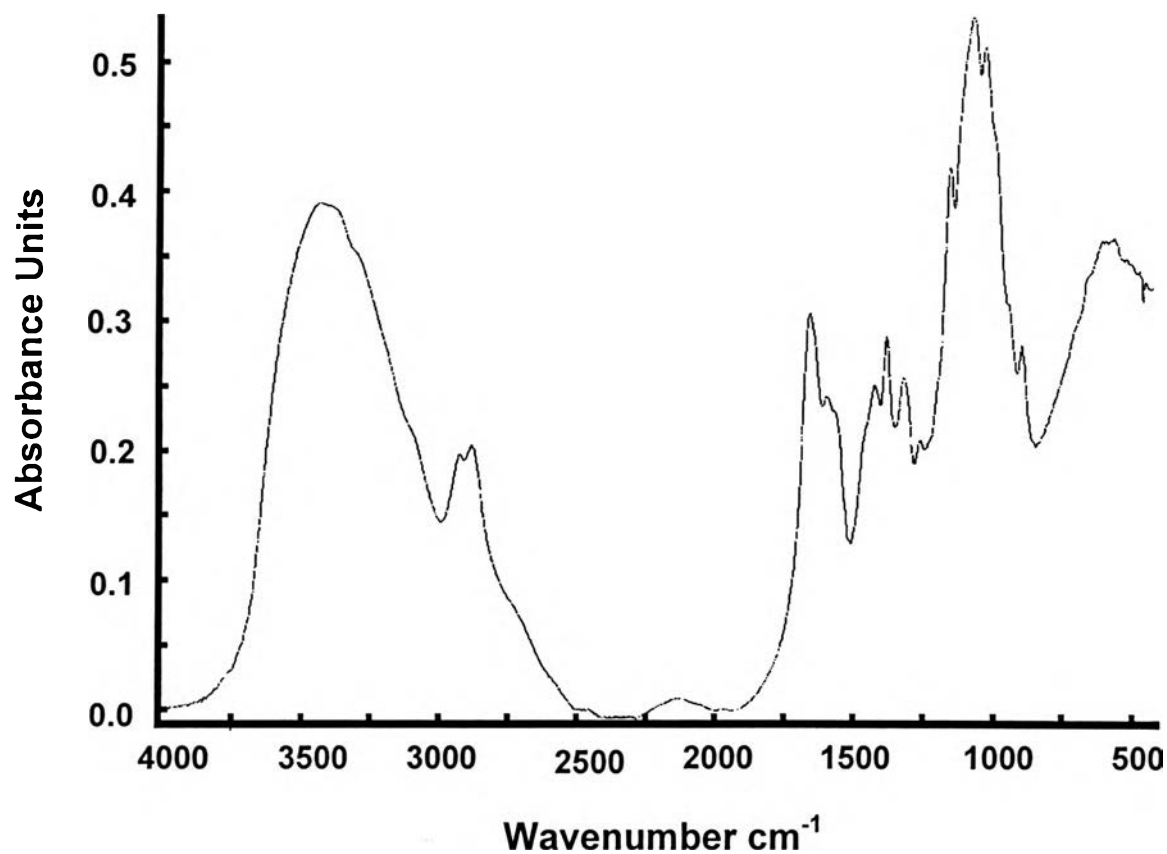
**Figure 4.2** FT-IR spectrum of chitosan (DD = 75.8%).

FT-IR (KBr, cm^{-1}) :- 3426 (O-H), 2881 (C-H), 1657,1560 (C=O

amide, 1598 (amine), 1073(pyranose rings).

The elemental analysis (EA) of chitosan % DD 85.9 and % DD 75.8 are as follows. Anal. Calcd. for $(C_6H_{11}NO_4)_{0.859}(C_8H_{13}NO_5)_{0.141}$: %C, 45.16; %H, 6.76; %N, 8.39. Found: %C, 40.41; %H, 7.73; %N, 8.99. Anal. Calcd. for $(C_6H_{11}NO_4)_{0.758}(C_8H_{13}NO_5)_{0.242}$: %C, 45.46; %H, 6.71 %N, 8.18. Found: %C, 37.39; % H, 6.85; %N, 9.07.

Generally, chitin-chitosan is a copolymer that cannot avoid the trace amount of mineral, especially $CaCO_3$, even from controlled extraction and purification process. Referred to specification of the starting material, the ash content of chitosan in % DD 85.9 and 75.8 is approximately 1-2 %. Thus, the EA results show the range differed from the calculated data. Concentration of N can be used as an internal standard according to the constant percent content from the chemical structure. In both cases, the found N percentage is close to that of the calculated data.
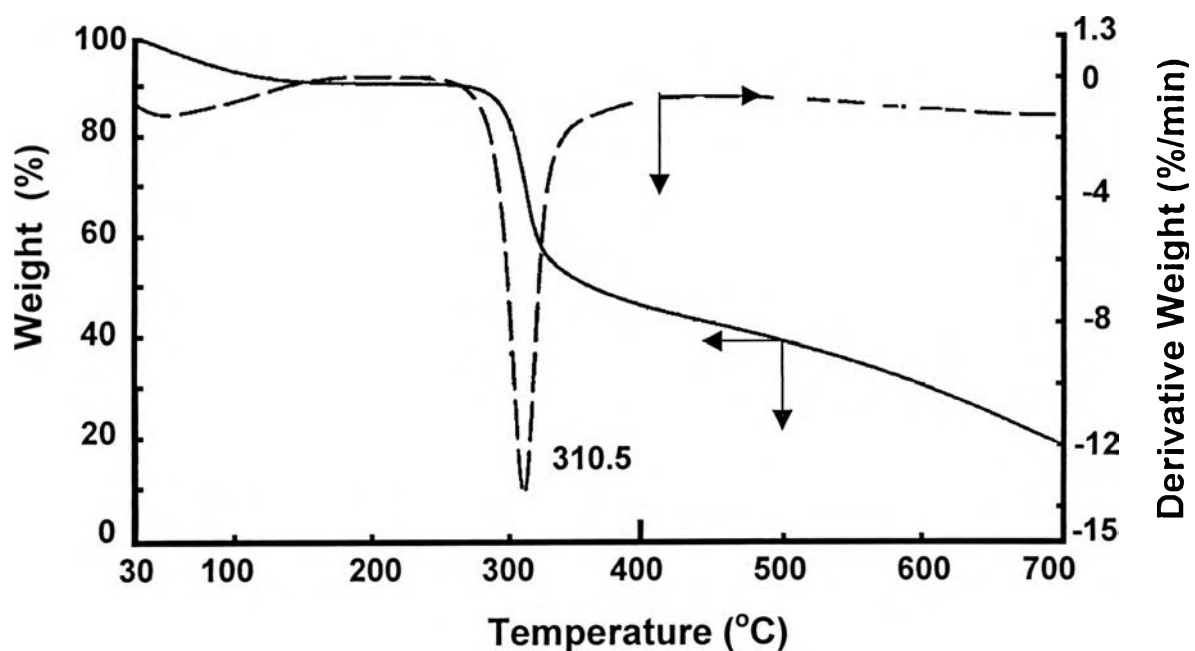
Figure 4.3 TGA diagram of chitosan with a degree of deacetylation 85.9%.
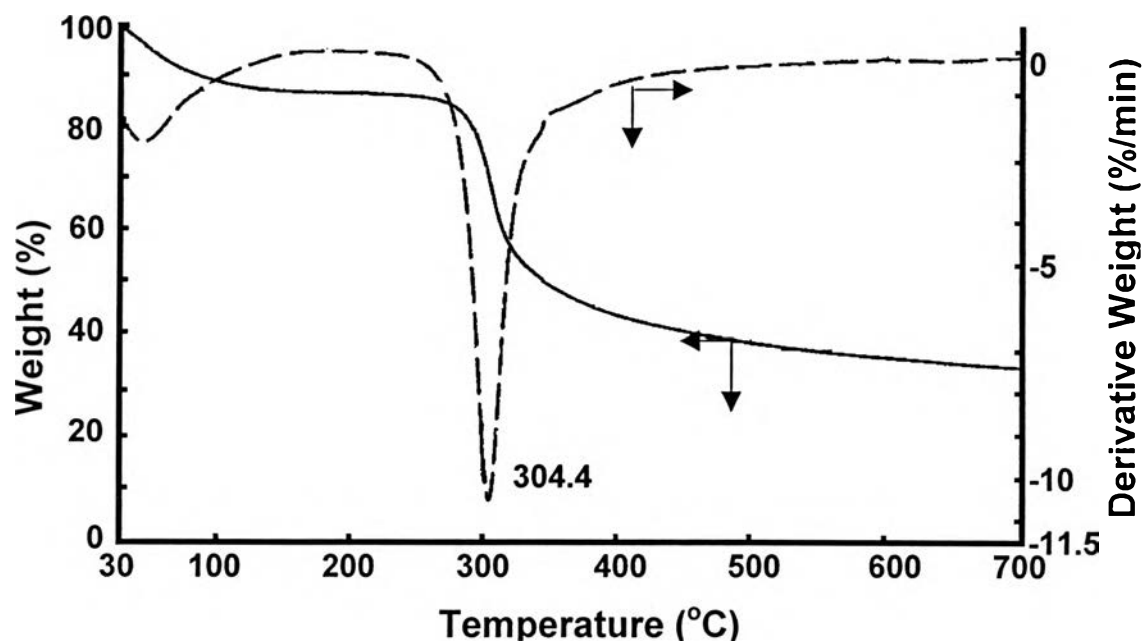
Figure 4.4 TGA diagram of chitosan with a degree of deacetylation 75.8%.

TGA of chitosan with the degree of deacetylation 85.9 % and 75.8% show the weight loss at 107.4°C and 86.3 °C, followed by the second peak at 310.5 °C and 304.4 °C, respectively (Figure 4.3-4.4). The former decay reveals the loss of moisture and water content in chitosan materials. The latter peak shows the degradation of chitosan, which may be owing to the bond breaking of glucoside linkage.

4.2 Preparation of Chitosan Precursors

The chemical conjugation of carbaryl onto chitosan is achieved by two molecular designs, i.e., carbaryl conjugated onto chitosan chain without and with a reactive spacer group to obtain a polymer drug for stability enhancement (Type 1) and for drug delivery system (Type 2), respectively. In the chitosan main chain, the hydroxyl and the amino groups are reactive

functional groups potentially available for chemical reactions. In order to achieve the proposed structure, chitosan was changed into a reactive precursor by focusing on chemically modifications at the C-6 position via two precursor pathways, 1. iodochitosan and 2. chitosan acetate-carbonyl imidazolide. Iodochitosan allows carbaryl conjugation directly onto the chitosan chain (Type 1). Chitosan acetate-carbonyl imidazolide (CA-CDI) has an ester spacer group, where carbaryl will couple onto chitosan via N,N'-carbonyldiimidazole.

4.2.1 Iodochitosan Pathway

Chitosan with a degree of deacetylation of 85.9 % was used as a starting material. Iodochitin can be obtained by iodination of tosylchitin, which is a potential reactive precursor as reported by Kurita *et al.* (1992). Thus, the preparation of iodochitosan is of interest to study the preparation of precursors for drug conjugation.

4.2.1.1 Preparation of Tosylchitosan

Tosylchitosan was prepared as reported by Tachaboonyakiat *et al.* (1998). The reaction was achieved under heterogeneous conditions at the interface. The success of the reaction was dependent on temperature control because of the rapid interfacial reaction. It was found that vigorous stirring at 0 °C in the initial stage was also a key factor in order to control the exothermal reaction (Kurita *et al.*, 1992).

The characterization by FT-IR was shown in Figure 4.5.
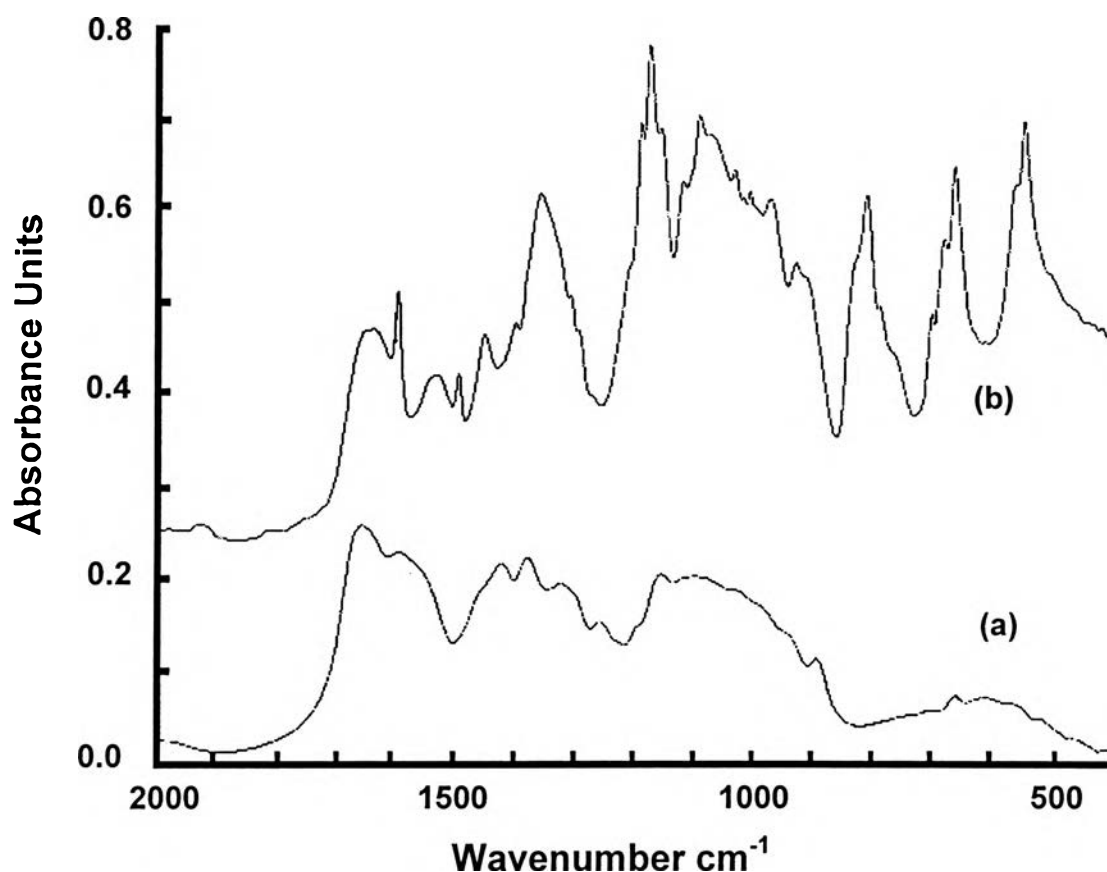
Figure 4.5 FT-IR spectra of (a) chitosan (DD = 85.9 %),

and (b) tosylchitosan.

FT-IR (KBr, cm^{-1}) :- 1657(C=O amide), 1598(p-phenylene),

1077 (pyranose rings), 1176 (tosyl group); 815 (p-phenylene).

The FT-IR spectrum shows a characteristic peak at 1176 cm^{-1} attributed to tosyl groups and the absorption bands at 1598 and 815 cm^{-1} due to p-phenylene groups.

The elemental analysis (EA) result is shown as follows:

Anal. Calcd. for $(C_{20}H_{23}NS_2O_8)_{0.859}(C_{15}H_{19}NSO_7)_{0.141}$: %C, 51.09; %H, 4.95; %N 3.09; %S 13.13. Found: %C, 47.53; %H, 5.97; %N, 4.38; %S 10.84.

Elemental analysis reveals significant sulfur content. The S/N ratio from the elemental analysis equals to 2.47 while the calculation from ideal

structure is about 4.25 (Figure 4.6). This implies that the reaction occurred about 58 % at either the hydroxyl or amino groups of chitosan.
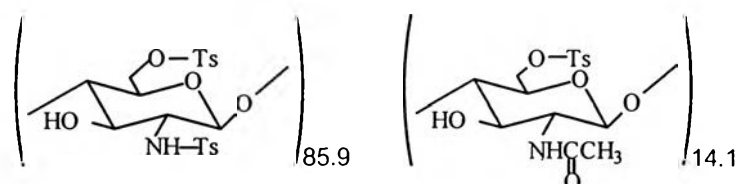
Figure 4.6 Ideal structure of tosylchitosan when tosylation

is completed to make the S/N ratio be 4.25.

TGA diagram of tosylchitosan is shown in Figure 4.7. The initial weight loss until 62.0 °C refers to the loss of moisture. By comparing these results to that of neat chitosan (Figure 4.4), the peak at around 193.3 °C evidently reveals the loss of tosyl groups while the latter peak at 304.4 °C is due to the breaking of glucoside linkages.
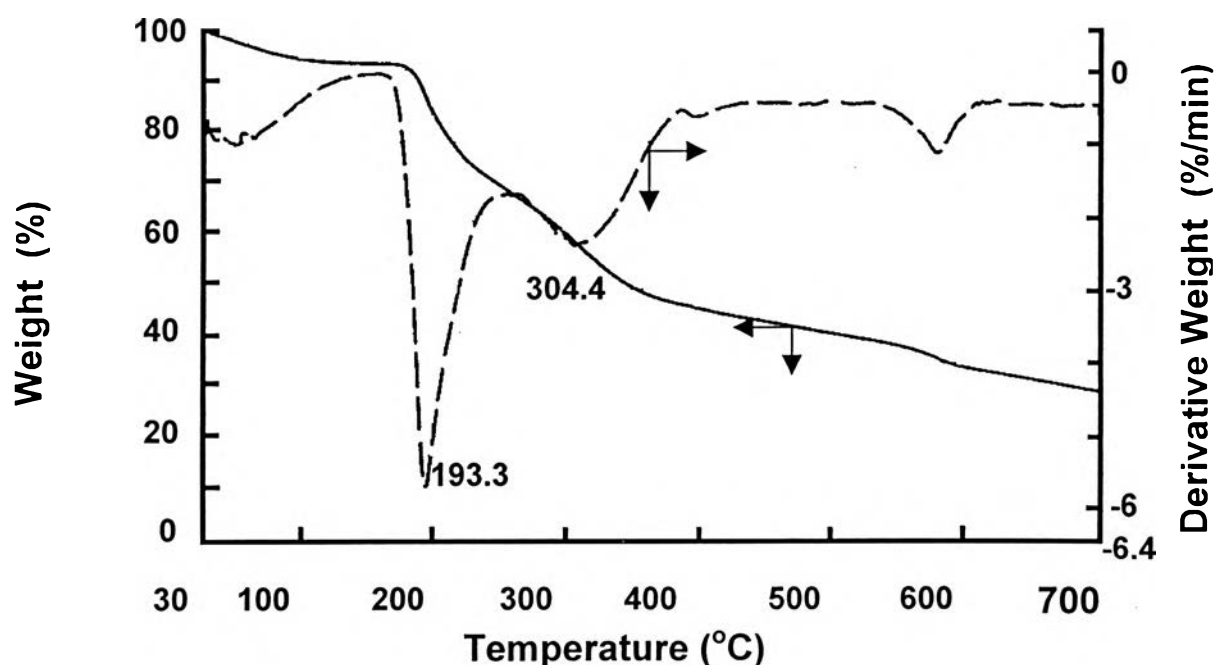
Figure 4.7 TGA diagram of tosylchitosan.

Solid state ^{13}C-NMR spectrum of tosylchitosan shows carbon peaks due to acetyl methyls and tosyl methyls at 21.99 ppm, pyranose rings at 54-100.34 ppm, aromatic rings at 129.98-145.16 ppm and carbonyl at 173.34 ppm (Figure 4.8). Thus, the NMR result confirms the successful synthesis of tosylchitosan.
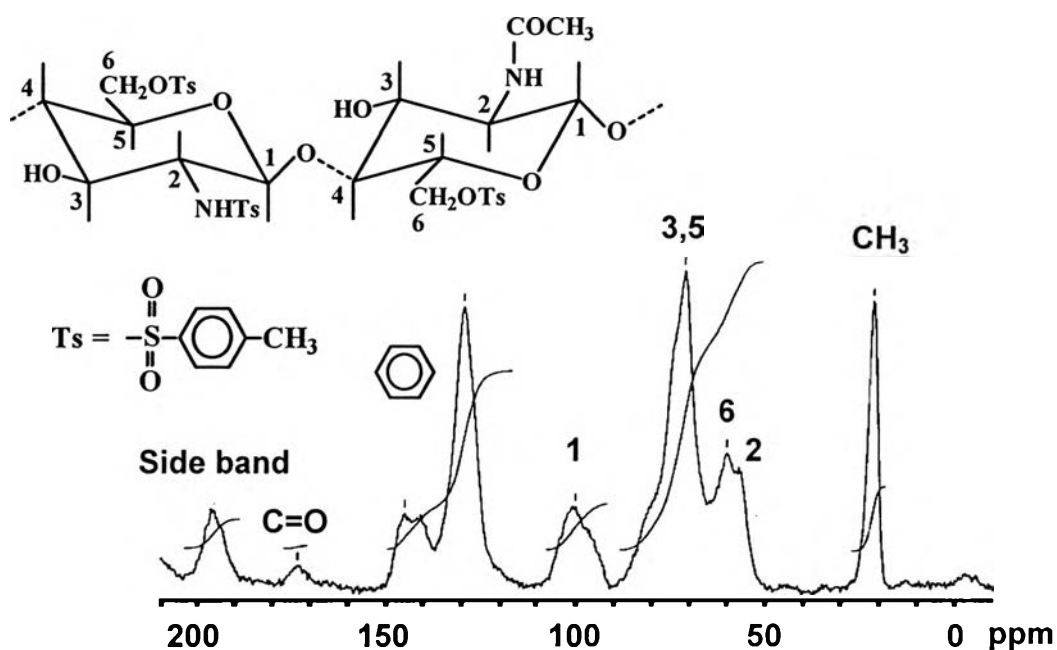

Figure 4.8 Solid state ^{13}C-NMR spectrum of tosylchitosan.

*4.2.1.2 Preparation of Iodochitosan*

The halogenated chitin derivative is expected to be a reactive precursor. In the present case, iodochitosan is of interest to obtain a drug molecule conjugated directly onto the chitosan chain (disscussed in 4.3.1).

Iodochitosan was prepared using the same procedure as iodochitin (*Kurita et al.*, 1992). The reaction was operated under heterogenous conditions at high temperature to enhance the efficiency of the reaction. The tosyl groups are substituted by the iodide ion of sodium iodide. Generally, the substitution takes place by either the S_N1 or S_N2 depending on the substrate, i.e., the alkyl group of alkyl tosylate (Wade, 1991). Theoretically, the S_N2

substitution of tosylchitosan (Scheme 4.1 (b)) is priority concerning with the primary alkyl group at the C-6 position. However, in the present case, the bulky group of chitosan will allow the reaction to proceed the intermediate and follow the S_N1 (Scheme 4.1 (a)). Though the mechanism cannot be confirmed, the FT-IR characteristic peak of tosyl group at 1176 cm^{-1} is decreased after reacted with NaI (Figure 4.9), suggesting that iodination was successful.
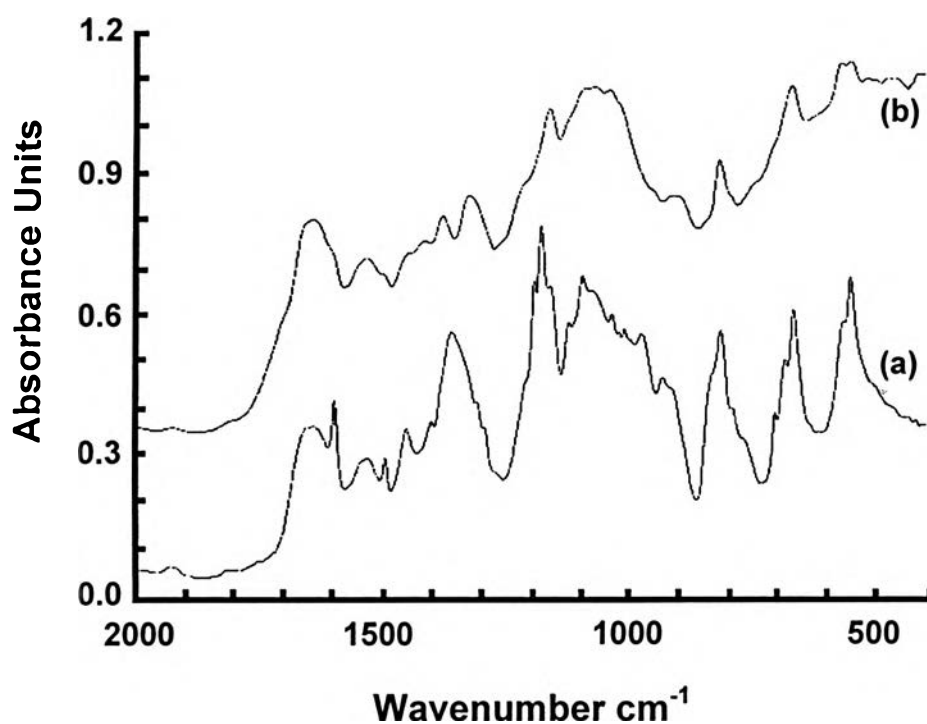
Figure 4.9 FT-IR spectra of (a) tosylchitosan, and (b) iodochitosan.
FT-IR (KBr, cm^{-1}) :- 1640, 1530 (C=O amide), 1067(pyranose rings).

(b)

(a)
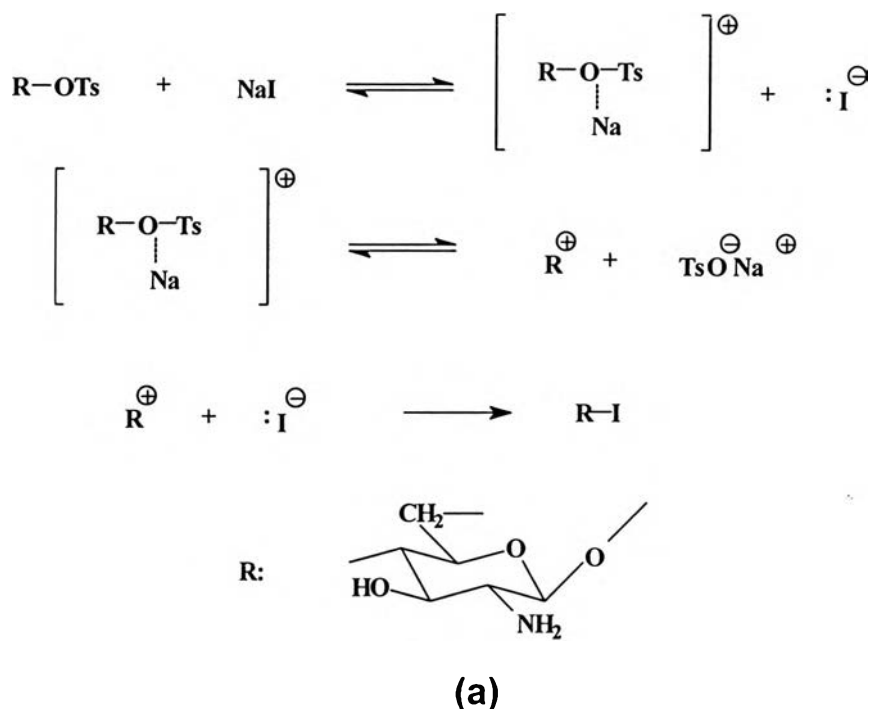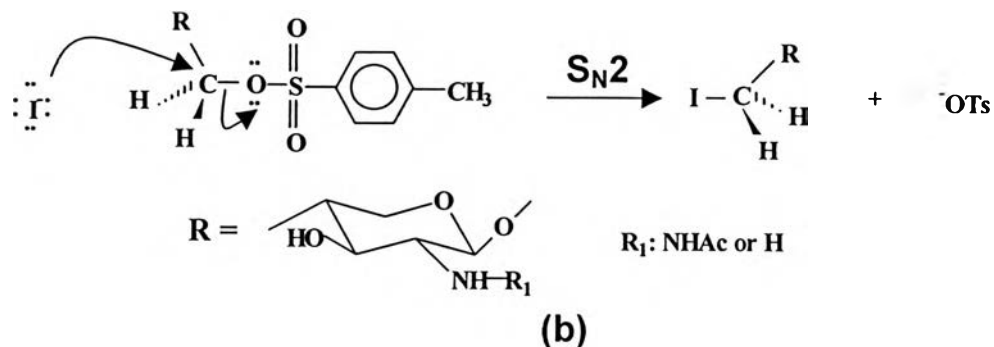
**Scheme 4.1** Iodination for tosylated chitosan by (a) S_N1 mechanism, and (b) S_N2 mechanism.

Normally, characteristic peaks of organohalogen compounds appear below 700 cm^{-1} which are difficult to observe due to the overlapping broad peaks of chitosan. Here, qualitative curve fitting techniques was applied to overcome the determination of the complex peak in the FT-IR spectra (Figure 4.10). It should be noted that the peak at 1699 cm^{-1} appears significantly

together with the decreasing tosyl peaks. Kurita *et al.* (1992) concluded the alkali treatment and iodination lead to the acetyl migration of chitin. However, the mechanism was not proposed. In the present case, the peak at 1699 cm^{-1} can be also considered as the result of acetyl migration. Here, the mechanism is proposed as the hydroxyl groups of chitosan changing to sodium alkoxide intermediate followed by attacking the chitin unit leading to acetyl migration (Scheme 4.2). This causes the degree of deacetylation of the modified chitosan to be higher than that of the starting material.

TGA diagrams of iodochitosan shows the weight loss at 216.6 $^{\circ}$C (Figure 4.11). By comparing these results to chitosan starting material which has peak loss at 310.5 $^{\circ}$C, it can be concluded that iodination leads to a decrease of thermal stability due to the bulkiness of the iodo group and repulsion between the iodochitosan chains.
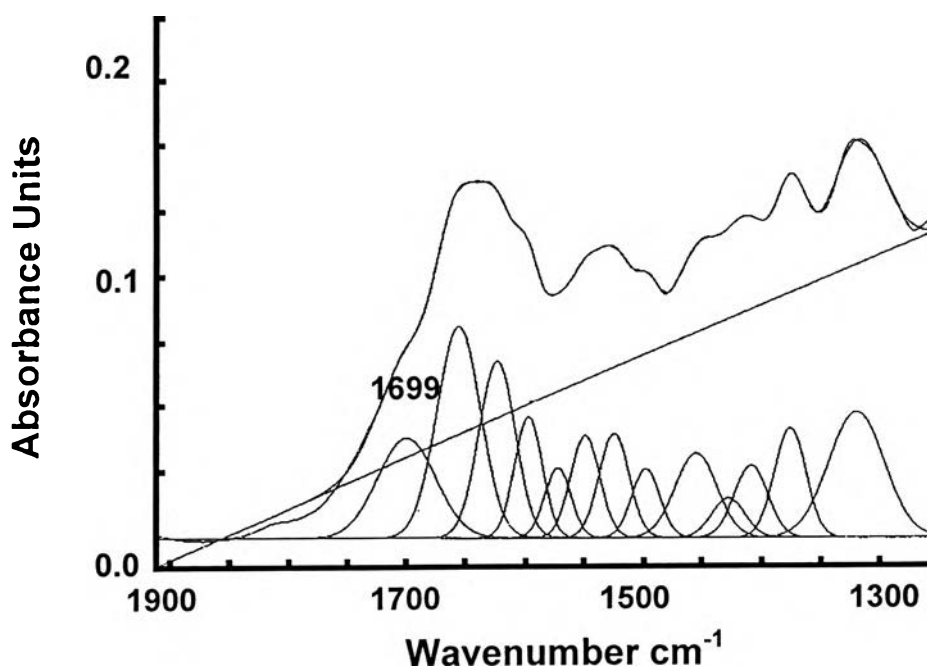
Figure 4.10 Qualitative curve fitting of iodochitosan.
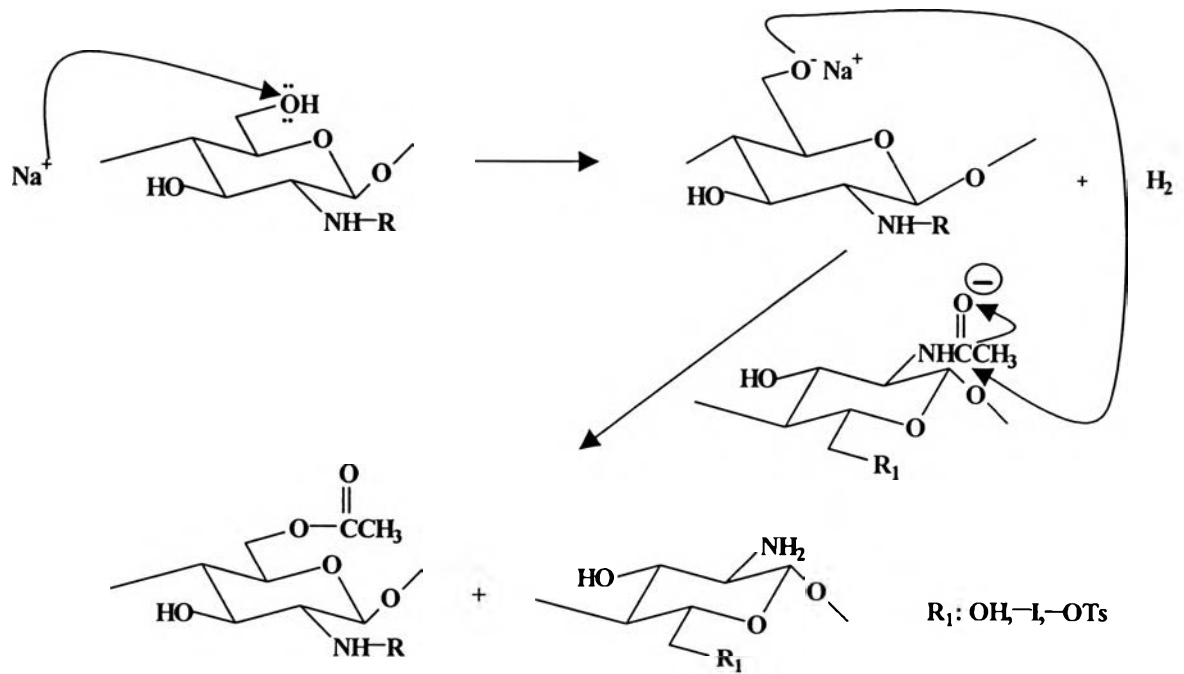
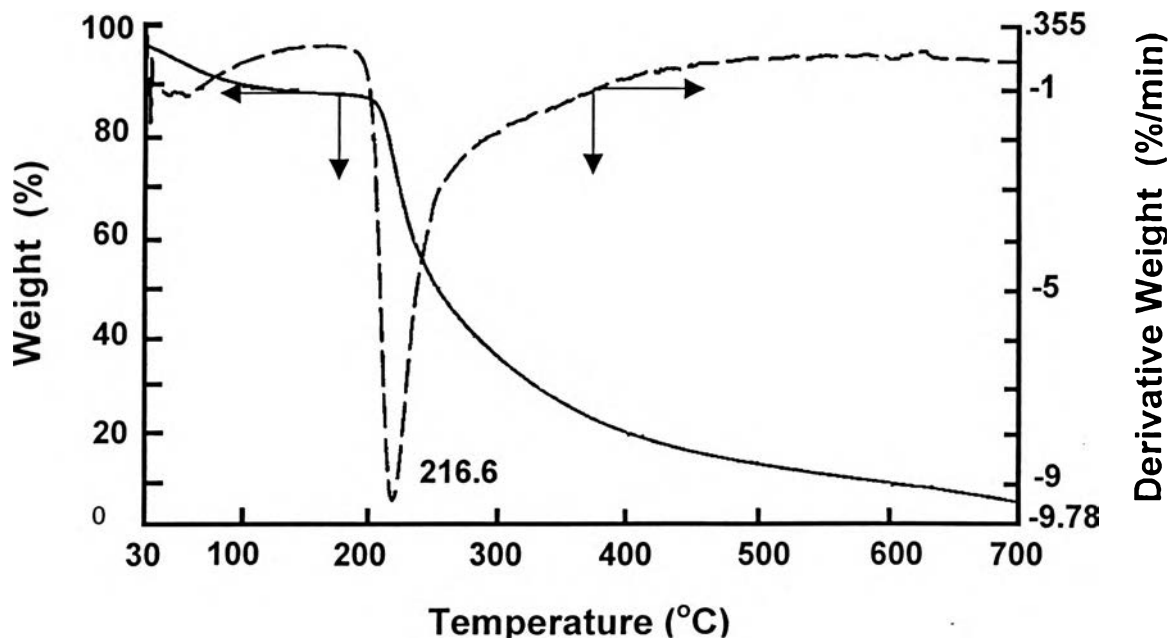**Scheme 4.2** Mechanism of acetyl migration on chitin unit

Figure 4.11 TGA diagram of iodochitosan.

4.2.2 Chitosan acetate-Carbonyl imidazolide (CA-CDI) Pathway

Chitosan with a degree of deacetylation of 75.8 % was used as a starting material.

4.2.2.1 Preparation of Chitosan acetate(CA)

An acetate salt was formed at the C-2 position to protect the amino groups and to allow further reaction between the hydroxyl groups at the C-6 position. The method is easy, inexpensive and able to avoid decreasing of molecular weight due to the mild reaction conditions. The FT-IR spectrum of chitosan acetate is similar to that of the chitosan starting material (Figure 4.12).
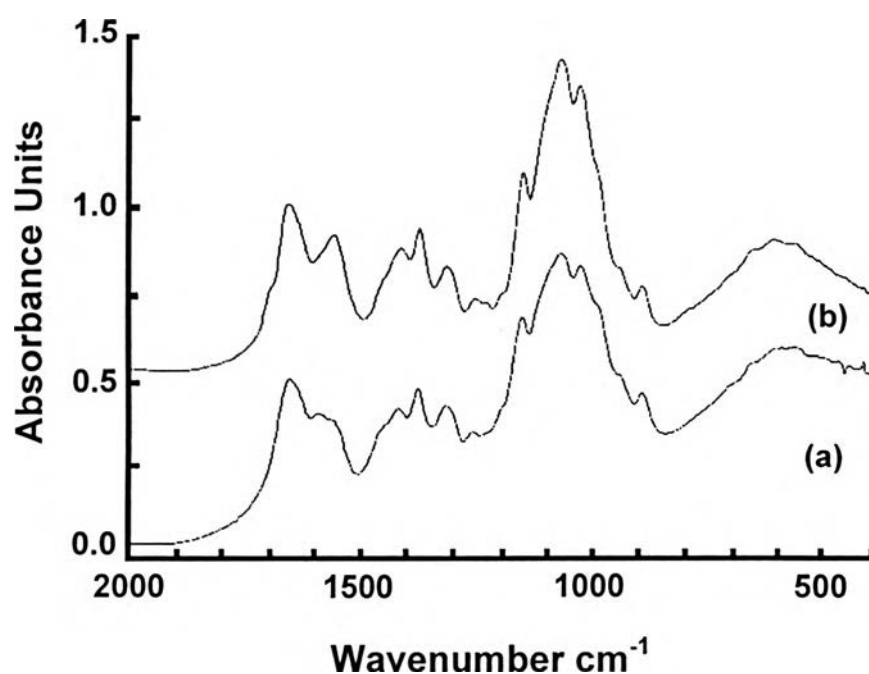
Figure 4.12 FT-IR spectra of (a) chitosan (DD =75.8%), and (b) CA. FT-IR (KBr, cm^{-1}): - 1662,1560 (amide),1073 (pyranose rings).

TGA reveals that there is the moisture absorbed in the derivatives as confirmed from the weight loss up to 73.2 $^{\circ}$C while the degradation peak at 292 $^{\circ}$C is close to that of chitosan starting material. These results also imply

that the chitosan salt formation does not significant influence the thermal stability (Figure 4.13).
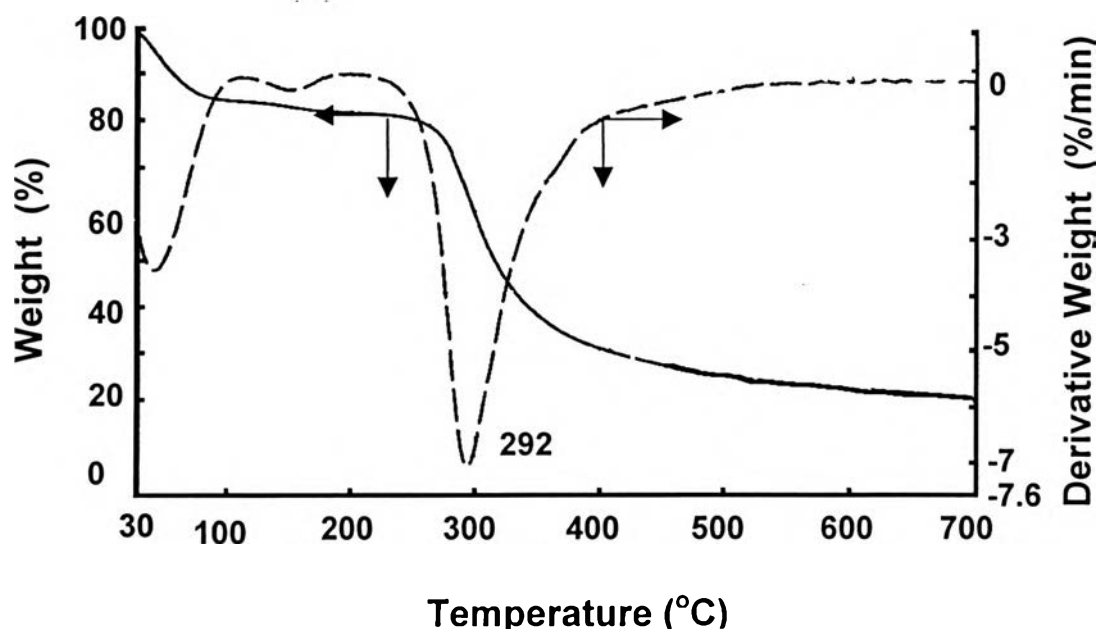
Figure 4.13 TGA diagram of chitosan acetate.

Preliminary elemental analysis of a well-defined chitosan found that chitosan acetate can be exceeded 80 %. Thus, chitosan acetate in this present work should have some amino groups remaining in the chitosan chain (Figure 4.14).
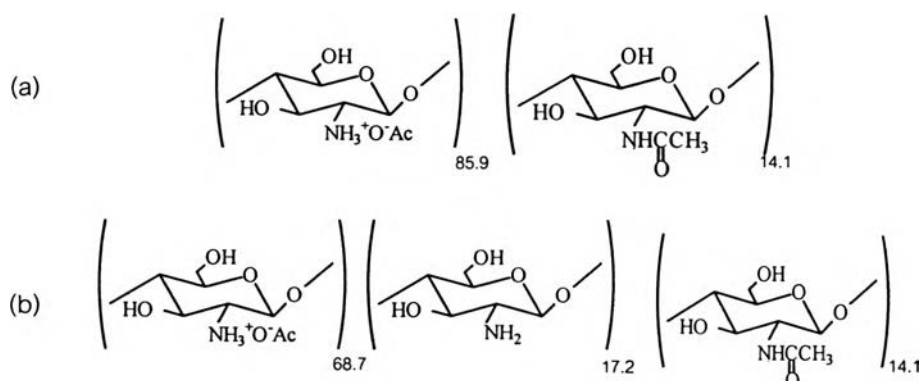
Figure 4.14 Structures of chitosan acetate from chitosan %DD = 85.9

(a) ideal structure for completion of acetate group, and

(b) 80 % acetate salt formation structure.

4.2.2.2 Synthesis of Chitosan acetate-Carbony imidazolide

    (CA-CDI)

The use of coupling agents is one approach for polymer-drug conjugation. The spacer formed by the coupling agent is a key factor for controlled release system. Dicyclohexylcarbodiimide (DCC) was reported to be an effective coupling agent for introducing chloramphenicol, a bioactive molecule into Biozan R$^{®}$ for drug delivery system (Simionescu *et al.*, 1985). *Chunharotrit et al.* (1998) reported that N,N'-carbonyldiimidazole (CDI) can be used to form activated ester as a spacer for the controlled release of chitosan conjugated chloramphenicol.

    Because of the high reactivity of N,N'-carbonyldiimidazole with alcohols, carboxylic acids, and amines, it is expected to be an effective coupling agent. However, to avoid complications, the amino groups at C-2 position of chitosan are protected in order to achieve chemically modification at only the C-6 position. The reaction condition also has to be limited to non-aqueous systems due to the degradation of CDI by water. Organic solvents such as N,N-dimethylformamide (DMF), N,N-dimethylacetamide (DMAc) are

possible. However, owing to the low solubility of chitosan in these solvents, the reaction has to be operated under herterogeneous conditions. Therefore, 4 moles equivalent to pyranose rings of CDI and severe conditions, i. e., 120 °C at the beginning of the reaction, were applied. Magnesium methoxide is also added as a catalyst for the reaction.

The ester of imidazolide shows a significant peak at over 1750 cm^{-1} as observed by FT-IR. As shown in Figure 4.15, the carbonylimidazolization is successful.
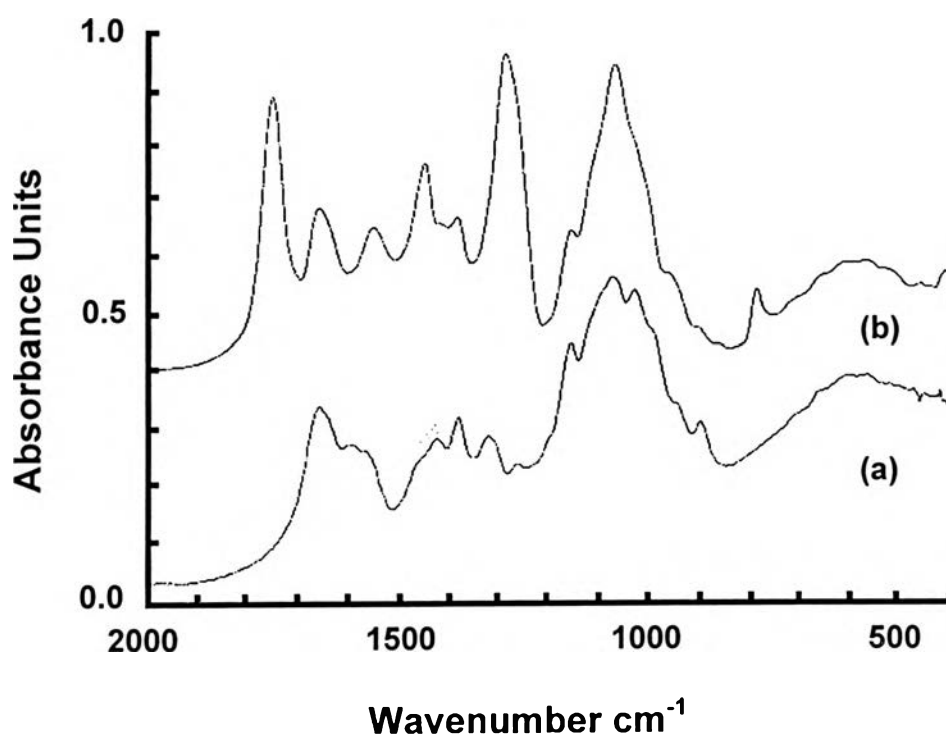
Figure. 4.15 FT-IR spectra of (a) chitosan acetate, and (b) CA-CDI.

FT-IR (KBr, cm^{-1}) :- 1659 (C=O amide),1752 (-COO- immidazolide)

1077(pyranose rings).

In another step, CA-CDI is used as a precursor. Thus, the peak characterization has to be operated clearly to be a reference for the next reactions. Here, qualitative FT-IR with curve fitting techniques was applied to distinguish the peaks (Figure 4.16). Curve fitting shows an ester peak at 1752 cm^{-1}, while amide II band appears as a shoulder at 1659 cm^{-1}. The pyranose band shows at 1077 cm^{-1} suggesting that the saccharide unit is not degraded by the reaction.
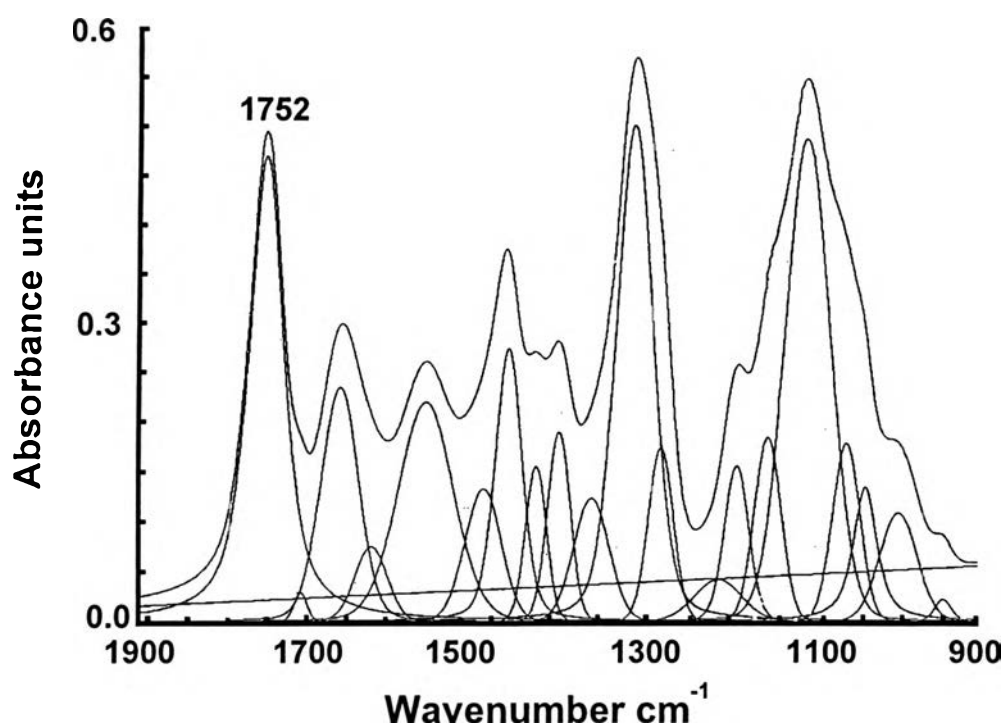
Figure 4.16 Qualitative curve fitting of CA-CDI.

The elemental analysis (EA) result is shown below:

Anal. Calcd. for $(C_{12}H_{17}N_3O_7)_{0.6064}$ $(C_{14}H_{15}N_5O_6)_{0.1516}$ $(C_{12}H_{15}N_3O_6)_{0.242}$: % C, 46.75; %H, 5.13; %N, 14.64. Found: %C, 41.06; %H, 5.38; %N, 8.23.

The calculation from ideal structure (Figure 4.17) gives the nitrogen content equal to 14.64 % while the found value shows only 8.23%. The result implies that carbonyldiimidazole (CDI) was introduced for 56.22 %.

Referred to the effective of acetate protecting step, the reaction can occur both at hydroxyl and unprotected amino unit.

60.64   15.16   24.20
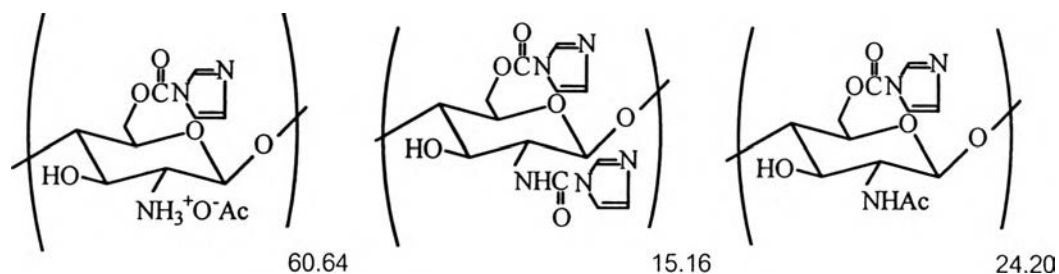
Figure 4.17 Ideal structure of chitosan acetate-carbonyl imidazolide of 80 % chitosan acetate formation.

Thermal studies reveal (Figure 4.18) that there is a new weight loss peak at 222.8 °C referring to the loss of CDI while the latter peak at 306.5 °C is the glucoside degradation. This further supports the successful introduction of CDI onto the chitosan chain.
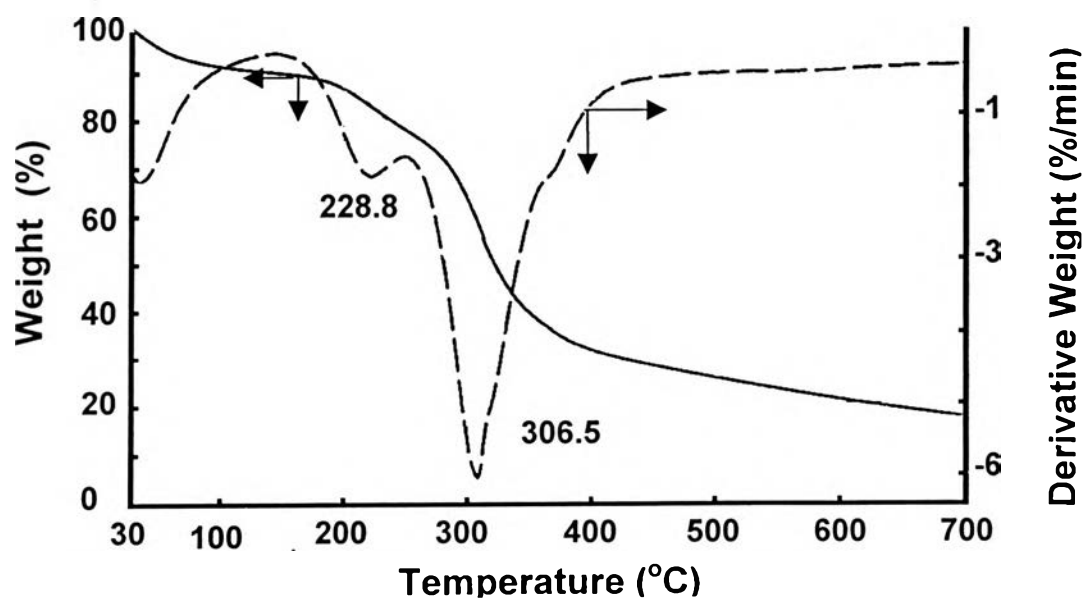
Figure 4.18 TGA diagram of CA-CDI.

Solid state ^{13}C-NMR was used to characterize the modified structure (Figure 4.19). Acetyl methyls carbons can be identified at 23.32 ppm, pyranose rings at 56.05-103.71 ppm, the carbonyl of CDI at 156.51 ppm, and chitin carbonyl at 173.38 ppm. The carbon of the imidazole is not observed, which may be due to insufficient relaxation time in the analysis. However, the peaks at around 60 ppm of the C-6 is found to be shifted to the lower field as a result of imidazolide conjugation leading to the overlapping of the peak with C-3 and C-5 peaks.
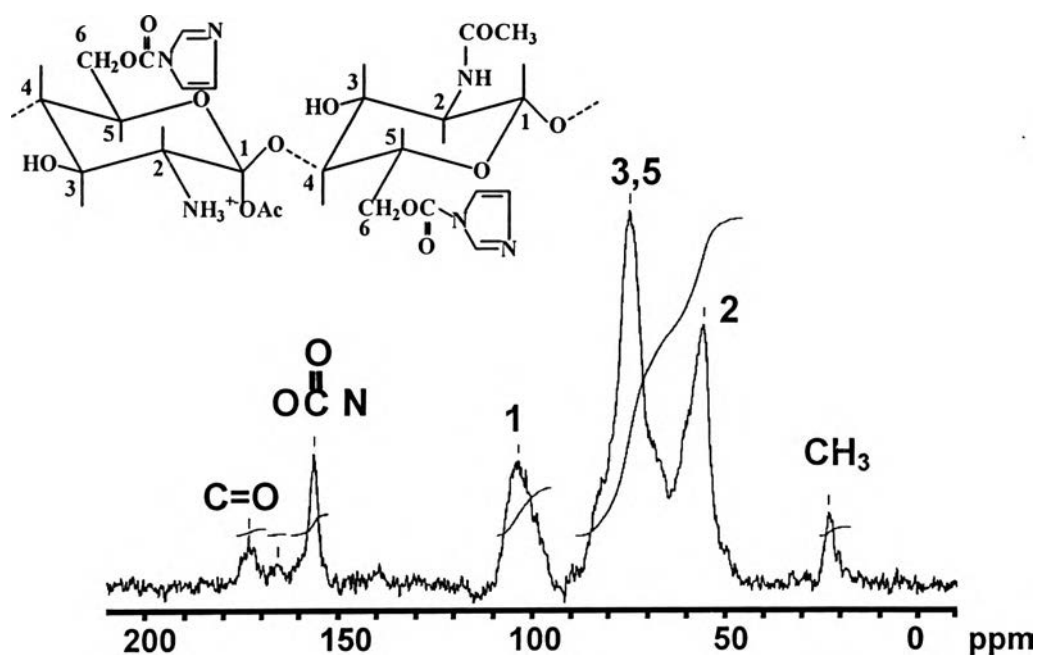

Figure 4.19 Solid state ^{13}C-NMR spectrum of CA-CDI.
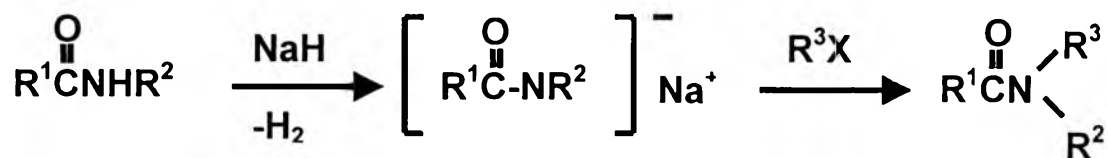
4.3 Preparation of Chitosan Conjugated Drug

Generally, the requirements of a model drug include the functional groups for the reaction, the effectiveness of the drug and the ease of drug characterization by analytical methods. The present work concerns applying a toxic drug, i.e., an insecticide, as a model drug for use as an agricultural controlled release system. 1-Naphthylcarbamate or carbaryl, CBR (Figure 4.20) was chosen due to its toxicity, low cost and problem of short application interval in practical use. Carbamate is suitable for its functional group, including the naphthyl ring as a chromophore for UV detection. The successful synthesis of the drug-conjugated compound also can be confirmed from the ester group belonging to carbamate easily by FT-IR.
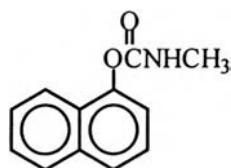
Figure 4.20 Chemical structure of carbaryl.

4.3.1 Synthesis of Chitosan Conjugated Drug Type 1: Chitosan-Carbaryl (CHI-CBR)

The polymer drug conjugation without spacer can be obtained by alkylation of alkylhalide. Carbamate groups cannot form complexes with chitosan or iodochitosan due to the low activity of secondary amide of carbamate. However, Fones alkylated the N-substituted amides by using sodium hydride (NaH) as a catalyst (Fones, 1949) as shown in Scheme 4.3. However, the reaction has to be carried out in a non-hydrolytic solvent. Normally, anhydrous benzene was used as a solvent. In this present work, to avoid the degradation of carbaryl, which will occur easily at high temperature and high basicity, the reaction was cooled at the beginning and NaH was added gradually.

$$R^1\overset{\overset{\displaystyle O}{\|}}{C}NHR^2 \xrightarrow[\text{-H}_2]{\text{NaH}} \left[R^1\overset{\overset{\displaystyle O}{\|}}{C}\text{-}NR^2 \right]^- Na^+ \xrightarrow{R^3X} R^1\overset{\overset{\displaystyle O}{\|}}{C}N\overset{\diagup R^3}{\diagdown R^2}$$

Scheme 4.3 Alkylation of N-substituted amides by using NaH (Fones,1949)

As shown in Figure 4.21 (b), the FT-IR spectrum shows a shoulder around 1700 cm^{-1} and the pyranose rings at 1086 cm^{-1} still remain in the polymer chain. This confirms that the degradation of chitosan has not occurred after treating the reaction with NaH as a catalyst.

The curve fitting analysis indicates the sharp peaks at 1707 cm^{-1} and 1648 cm^{-1} owing to the ester of carbamate and tertiary amide, respectively, confirming the existence of carbaryl on chitosan chain (Figure 4.22).

The TGA diagram of CHI-CBR (Figure 4.23) shows a loss of moisture until 89.2 °C. The mass loss at 221.5 °C might relate to the stability of the polymer drug, which is less than that of pure chitosan. This can be associated with the bulky groups of the drug molecules interfering the molecular packing, which decreases the thermal stability.
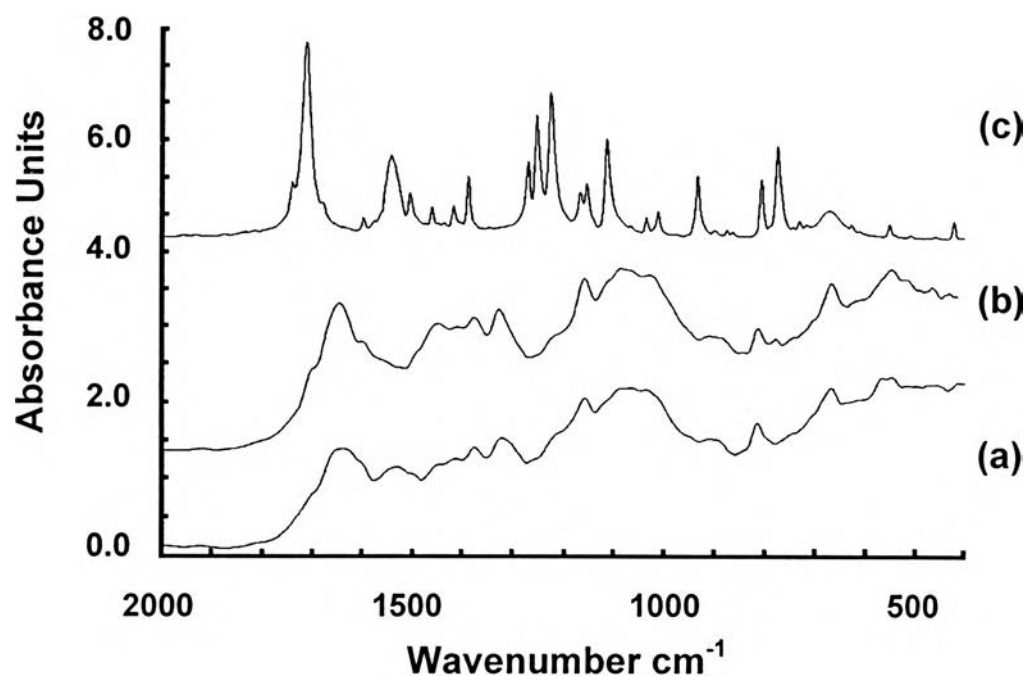
Figure 4.21 FT-IR spectra of (a) iodochitosan, (b) CHI-CBR, and (c) carbaryl.

FT-IR (KBr, cm^{-1}) :- 1647 (C=O),1086(pyranose rings).
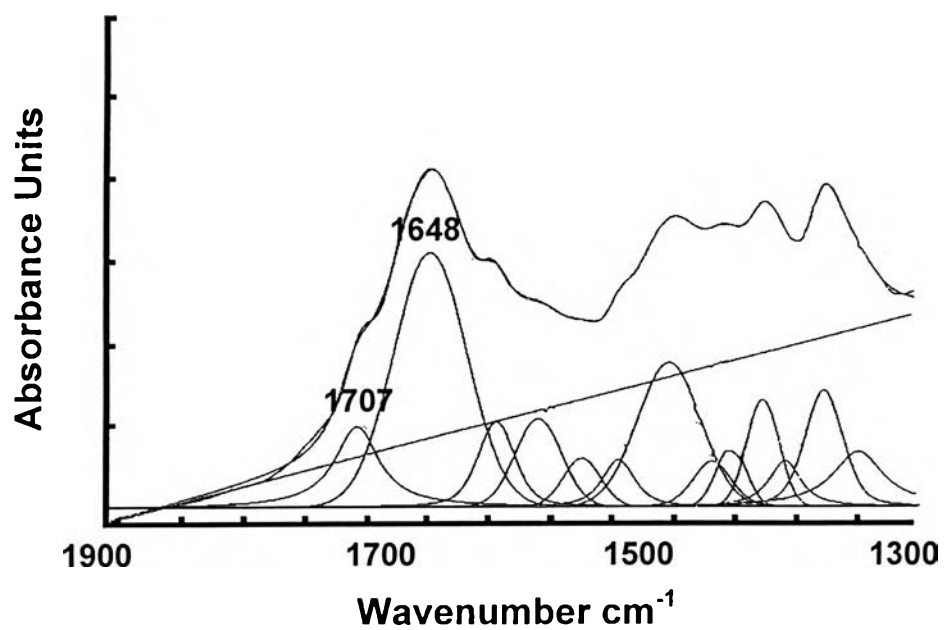
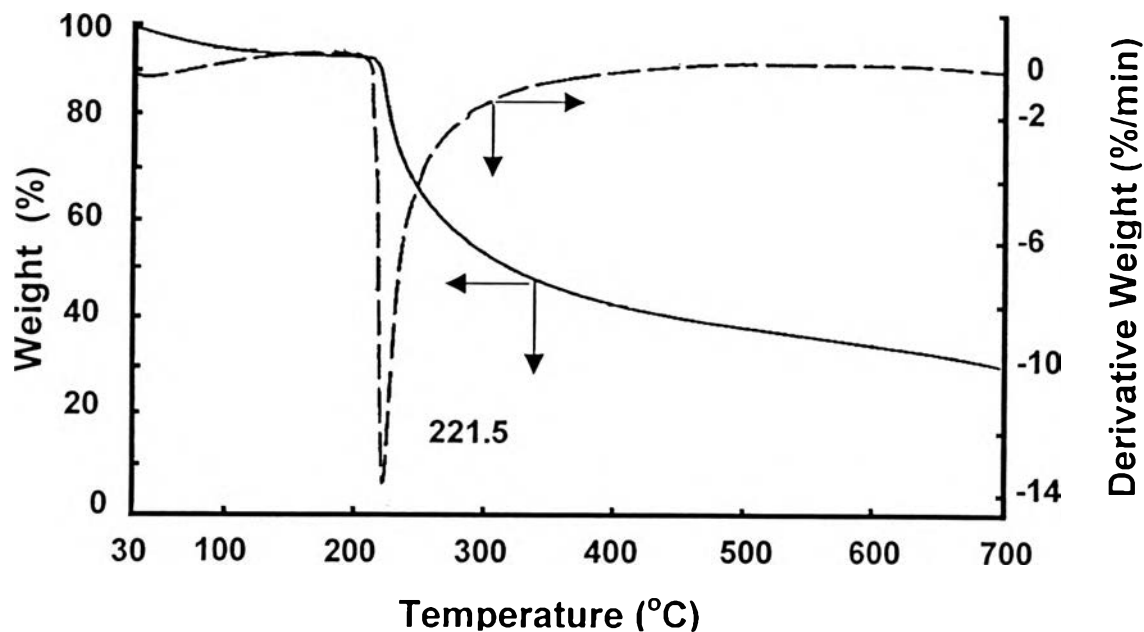**Figure 4.22** Qualitative curve fitting of CHI-CBR.

Figure 4.23 TGA diagram of CHI-CBR.

4.3.2 Synthesis of Chitosan Conjugated Drug Type2: Chitosan acetate-Carbonyl imidazolide-Carbaryl (CA-CDI-CBR)

Due to the low activity of secondary amide of carbamate ester, the reaction for carbaryl conjugated with chitosan via spacer cannot be achieved easily even with the high reactivity of chitosan imidazolide. To overcome this problem, a similar approach has been used to alkylate N-substituted amides (Fones, 1949). Sodium hydride was applied as a catalyst for changing carbaryl into a reactive nucleophile before reacting with chitosan imidazolide precursor as for the mechanism shown in Scheme 4.4.
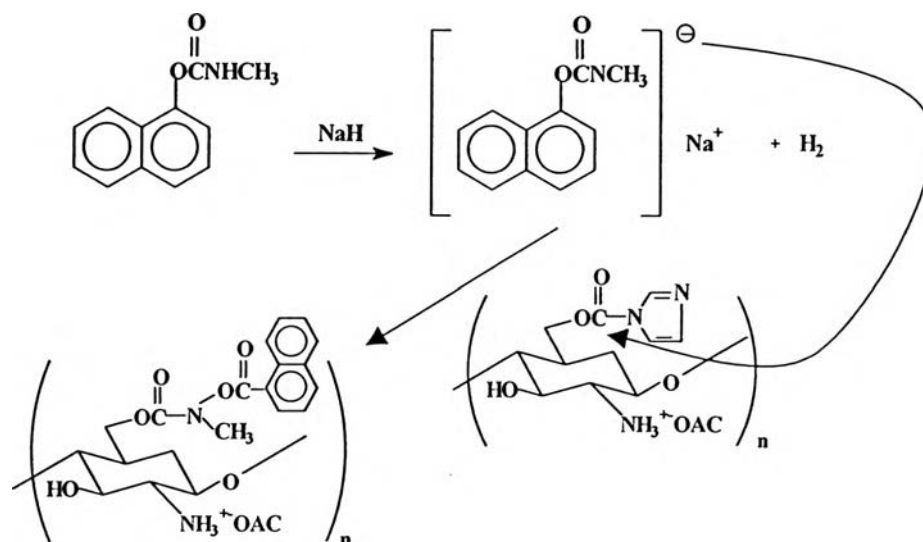
Scheme 4.4 Mechanism of carbaryl coupling onto
chitosan acetate-carbonyl imidazolide

As shown in Figure 4.24, the absorbance at 1752 cm^{-1} of the imidazolide is decreased whereas a new peak occurs at 1708 cm^{-1}. The characteristic pyranose rings peaks still remained. This indicates that some ester of CDI was substituted by carbaryl without the degradation of chitosan main chain.
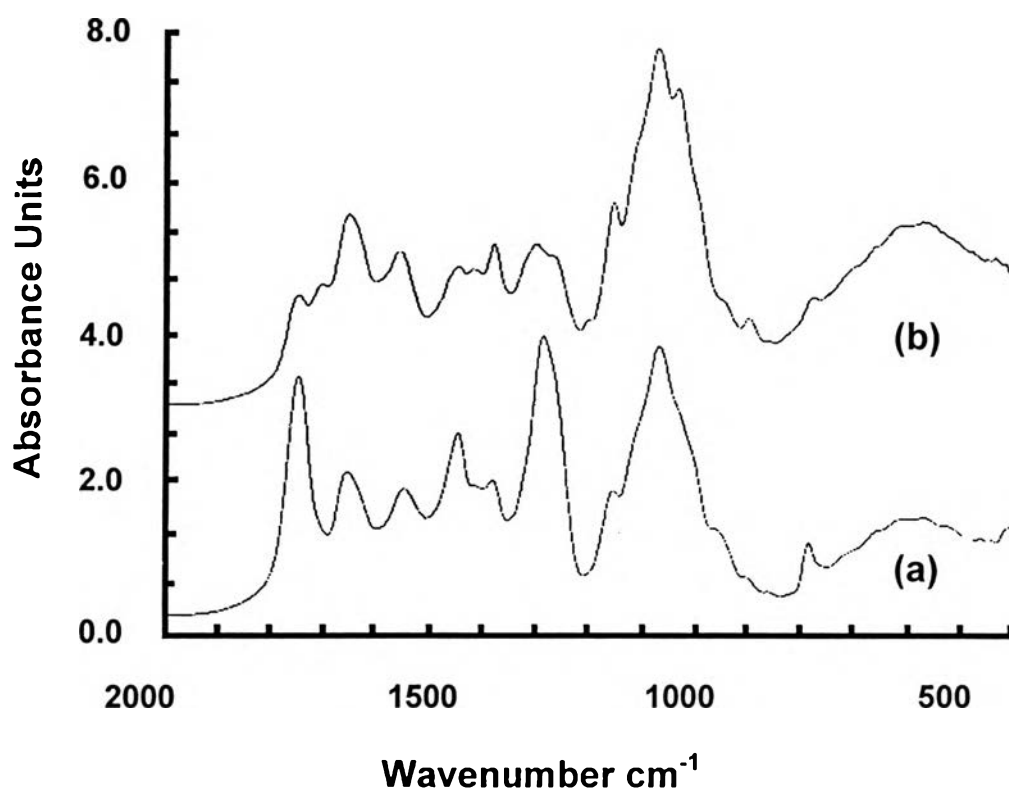
Figure 4.24 FT-IR spectra of (a) CA-CDI, and (b) CA-CDI-CBR.
FTIR (KBr, cm^{-1}) :- 1752 (-COO- immidazolide), 1708 (-COO-
carbamate), 1657 (C=O amide), 1071(pyranose rings).

The curve fitting result confirms the achievement of the reaction by
the peak at 1708 cm^{-1} of carbamate ester (Figure 4.25).

TGA shows the weight loss of moisture or residual solvent until
61.6 °C. The degradation of the polymer drug is similar to that of chitosan
starting material or the precursor. However, the polymer drug exhibits a
broader peak starting from 158 °C to 345 °C, which maybe included the loss of
carbaryl. It should be noted that the weight loss peak of carbaryl at its melting
point of 142 °C cannot be observed in the polymer drug. Here, the coupling
onto chitosan main chain makes the carbaryl become thermally stable as a
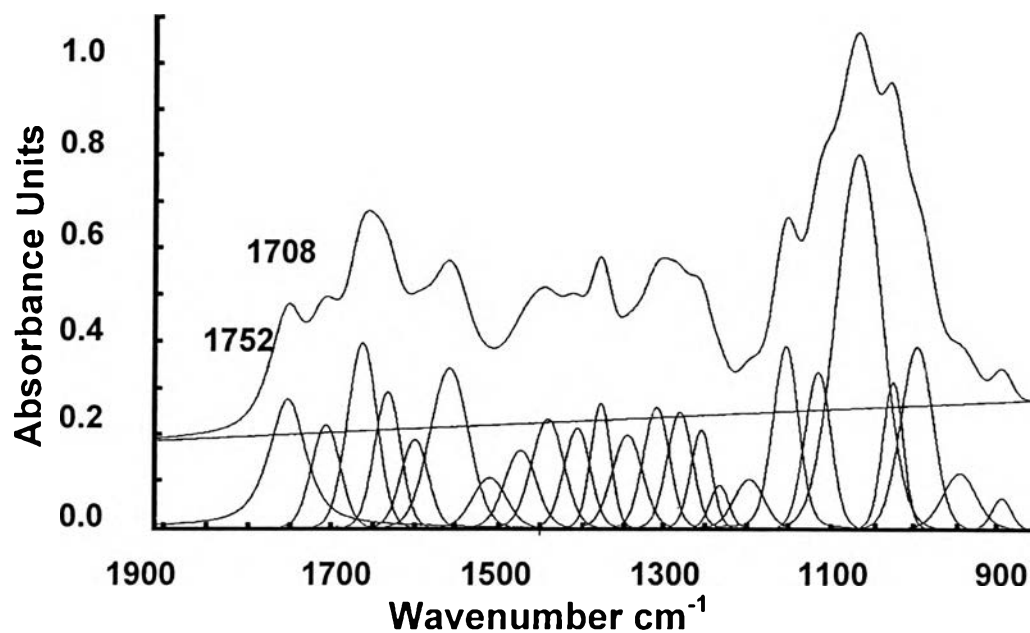result of chitosan main chain (Figure 4.26).

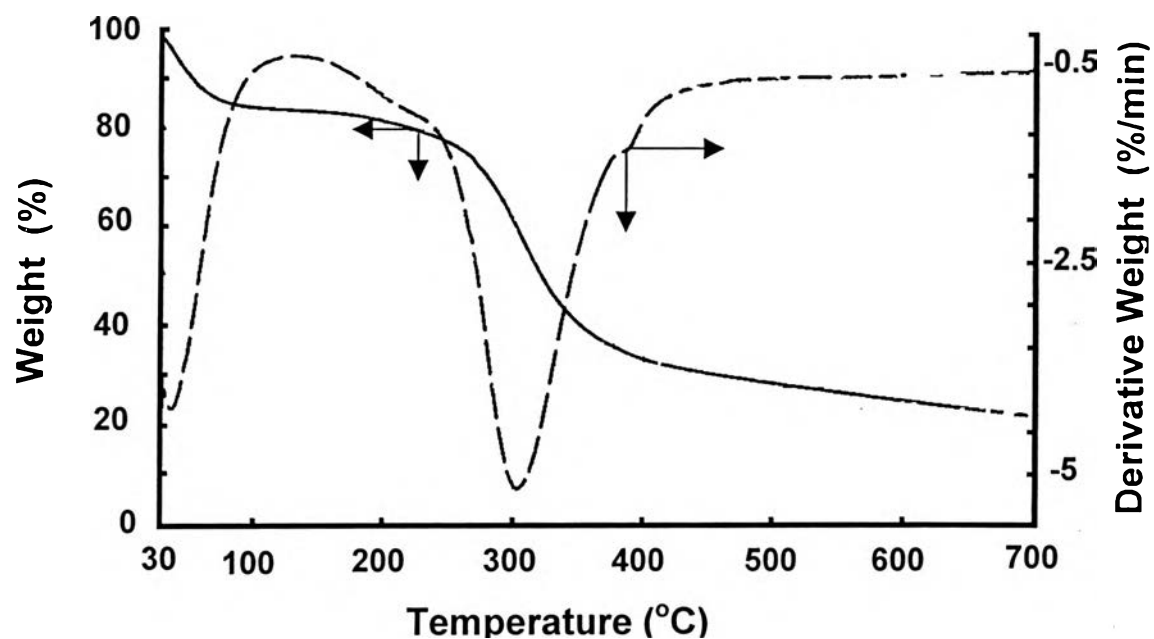**Figure 4.25** Qualitative curve fitting of CA-CDI-CBR.

Figure 4.26 TGA diagram of CA-CDI-CBR.

4.4 Structural Study by XRD

In order to evaluate chitosan structure related to chemical conjugation, powder XRD has been studied. Takai *et al.* (1988) reported that crab shell chitosan forms as orthorhombic α-chitin with major peaks at around 19° with the subsidiary peaks at 9° and 20°. In the present work, shrimp shell chitosan starting materials with the degree of deacetylation 85.9 and 75.8 showed peaks at 9.42°, 19.64° and 9.18°, 19.66°, respectively (Figure 4.27).

4.4.1 Structural Analysis of Type 1: Chitosan-Carbaryl (CHI-CBR)

In the case of chitosan of Type 1 drug conjugation, chitosan has been modified in 3 steps, i.e., tosylchitosan, iodochitosan and CHI-CBR. As shown in Figure 4.28, it is found that after the first step for tosylchitosan, the peaks are broader and shifted to lower values of 2θ. This implies a decrease in the crystalline, which may be due to the bulky tosyl groups interfering with the packing of the order chains. In the case of iodochitosan, it is found that the correlation length (D value) is much less than that of chitosan starting material, i.e., D of iodochitosan = 20 Angstroms, D of chitosan = 50 Angstroms. This suggests the distortion in the structure as known to be mosaic crystal structure. The elemental analysis shows that the successful of each reaction is in the range of 50-60 % (see 4.2.2.2). Here, the XRD results also support that there are several chitosan units in the structure, i.e., chitosan, tosylchitosan, and iodochitosan units in the chitosan main chain. In the case of final product, carbaryl conjugated chitosan, two characteristic broad peaks at 2θ of 10° and 20° are found with a small correlation length, (D=20 Angstroms), which should be referred to the combination of various units in chitosan main chain with the distortion of the crystal unit.

4.4.2 Structural Analysis of Type 2: Chitosan acetate-Carbonyl imidazolide (CA-CDI-CBR)

Comparing the chitosan starting material for type 1 which is mainly chitosan chain, with the starting material of type 2 (%DD = 75.8) (Figure 4.27) shows that the chitosan for type 1 has a higher correlation length (D =50 Angstroms) than that of type 2 (D =33.33 Angstroms). Chitosan acetate shows 2θ positions similar to chitosan as shown in Figures 4.29 (a) and (b). However, the peaks are much broader, indicating the crystal distortion as a result from the salt formation. The XRD result reflects the thermal analysis data, which shows a wide range of the degradation temperature than that of the starting chitosan. In the case of CA-CDI, a broader peak from $18.1°\sim23.5°$ is found (Figure 4.29 (c)). The d spacing of CA-CDI is found to be close to chitosan acetate (d = 4.43 for CA and d = 4.55 for CA-CDI). Elemental analysis reveals that the extent of the reaction is approximately 50 %, which refers to the amount of the unit with CDI linked to chitosan. Thus, it can be concluded that the chemical modification of CDI shows less effect on crystal structure with the similar mosaic structure. The XRD of CA-CDI-CBR (Figure 4.29 (d)) shows similar pattern as type 1(Figure 4.28 (d)).

In overall, by combining the XRD result with the thermal analysis, it is found that by chemical modification, chitosan loses the crystallinity to be a distorted structure, which reflects to the decrease of degradation temperature.
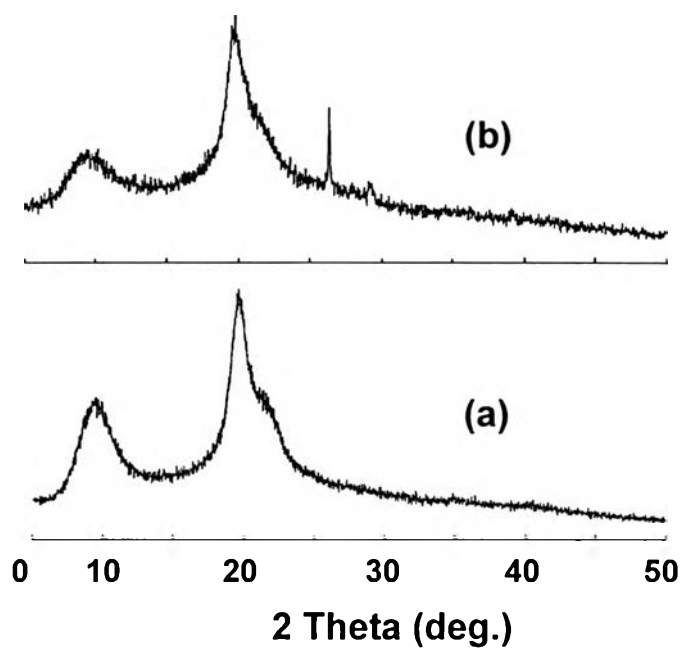
Figure 4.27 XRD patterns of chitosans (a) DD = 85.9 %, and
(b) DD = 75.8 %.
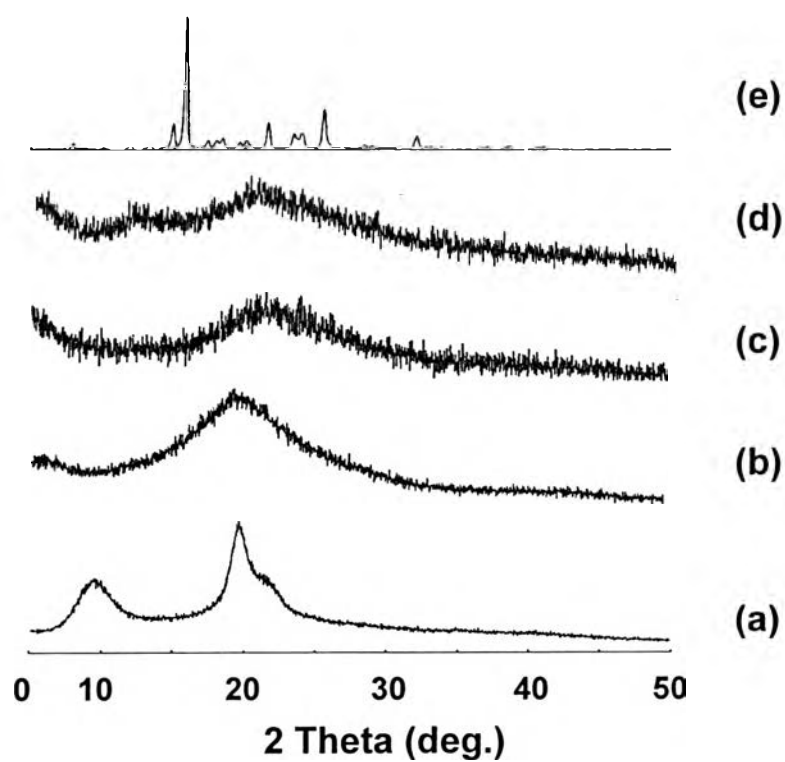
Figure 4.28 XRD patterns of (a) chitosan (DD =85.9 %),
(b) tosylchitosan, (c) iodochitosan, (d) CHI-CBR, and (e) carbaryl.
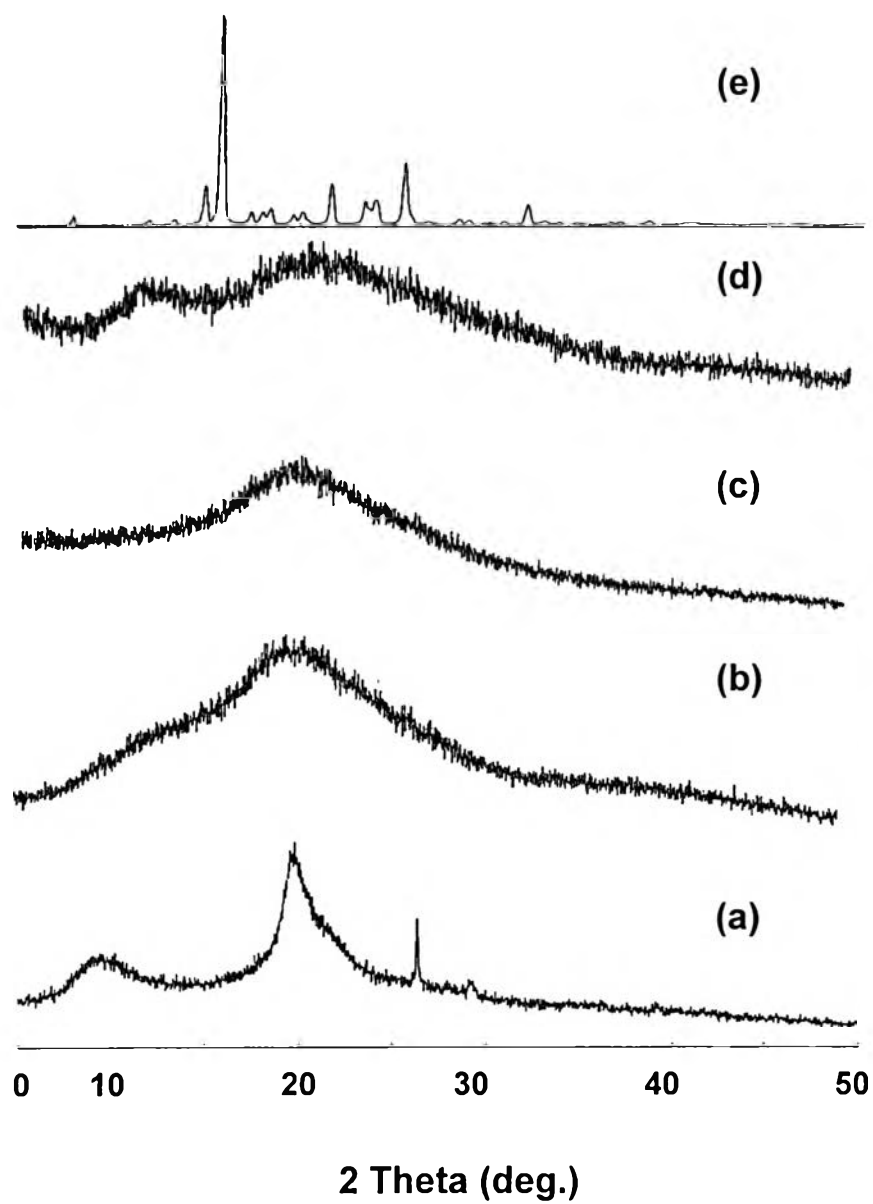
Figure 4.29 XRD patterns of (a) chitosan (DD = 75.8 %), (b) CA, (c) CA-CDI, (d) CA-CDI-CBR, and (e) carbaryl.

4.5 Stability Study of Chitosan Conjugated Drug Type 1: Chitosan-Carbaryl (CHI-CBR)

Carbaryl is known to be degraded in alkali conditions to naphthol derivatives (Worthing, 1979).

The present approach aims for a stable drug by directly bonding carbaryl onto chitosan. Thus, it is our interest to study the degradation of the carbaryl and compare these results to the obtained compound. In the present case, the carbaryl and chitosan-carbaryl were studied in alkali solution at pH 12 at 60 °C for 2 hours. Figure 4.30 reveals that the carbaryl is degraded in this condition to show the peaks at 209, 245 and 331 nm which correspond to the napthol derivative (Figure 4.30 (b)). In the same condition, however, chitosan-carbaryl is found to be stable because those peaks of carbaryl and napthol cannot be observed. Here, it should be noted that the UV peaks appear at 195 and 224 nm (Figure 4.30 (c)). These peaks of sodium iodide can be compared to as Figure 4.30 (d). This indicates a limitation of the coupling with the remaining iodochitosan, and the stabilization of carbaryl. A schematic drawing (Figure 4.31) is presented to explain the protection of the chain for carbaryl under severe reaction conditions.
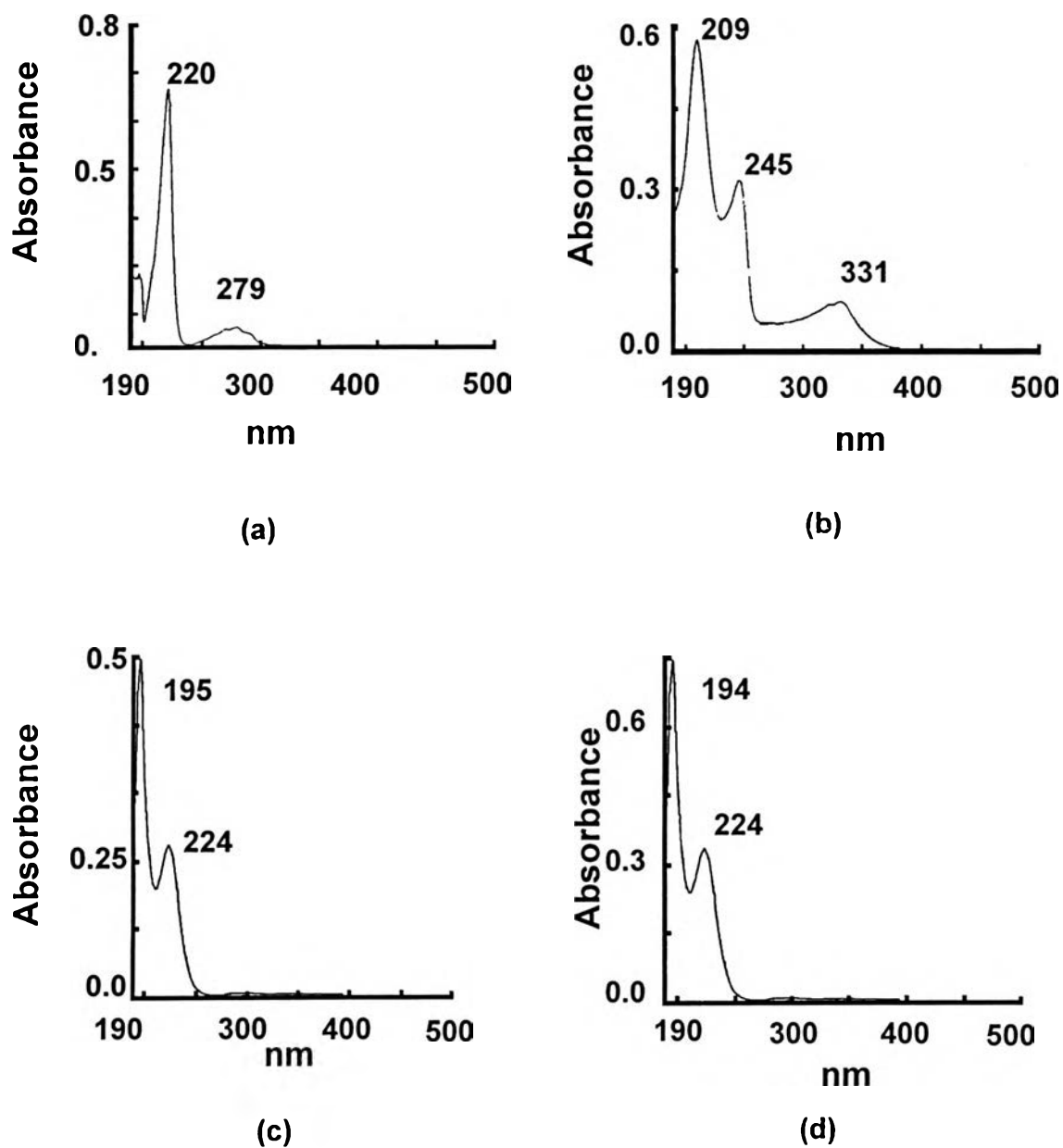
Figure 4.30 UV spectra of (a) carbaryl in methanol, (b) carbaryl in

0.01 N NaOH at 60°C for 2 h, (c) CHI-CBR in 0.01 N

NaOH at 60°C for 2 h, and (d) NaI in 0.01 N NaOH.
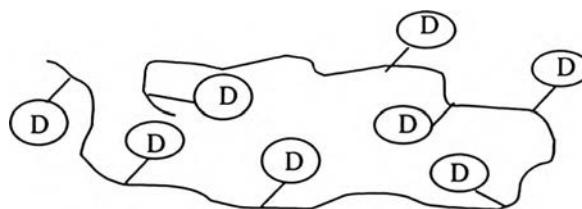
Figure 4.31 Polymer chain as a protector for polymer drug as a stable drug.

4.6 Release Study of Chitosan Conjugated Drug Type 2: Chitosan acetate-Carbonyl imidazolide-Carbaryl (CA-CDI-CBR)

Normally, the controlled release of the conjugated polymer drug with ester spacers can be achieved by the hydrolysis either by acid or base catalyst (Chunharotrit *et.al.*, 1998). In this work, by considering the CA-CDI-CBR structure, the release can be occurred either at the ester of CDI spacer to obtain carbaryl, or at the carbamate ester of carbaryl to obtain naphthol (Figure 4.32). A study was done under severe conditions to investigate the release in a certain time. The release of CA-CDI-CBR at 60 °C for 0.5 hour is found to be achieved by the hydrolysis at the CDI ester spacer position because the UV peaks indicate that the product released is carbaryl (Figure 4.33, Figure 4.30 (a)). Thus, it can be concluded that the hydrolysis occurs at reactive ester of spacer rather than at the stable carbamate ester. As a result, the controlled release has been accomplished.
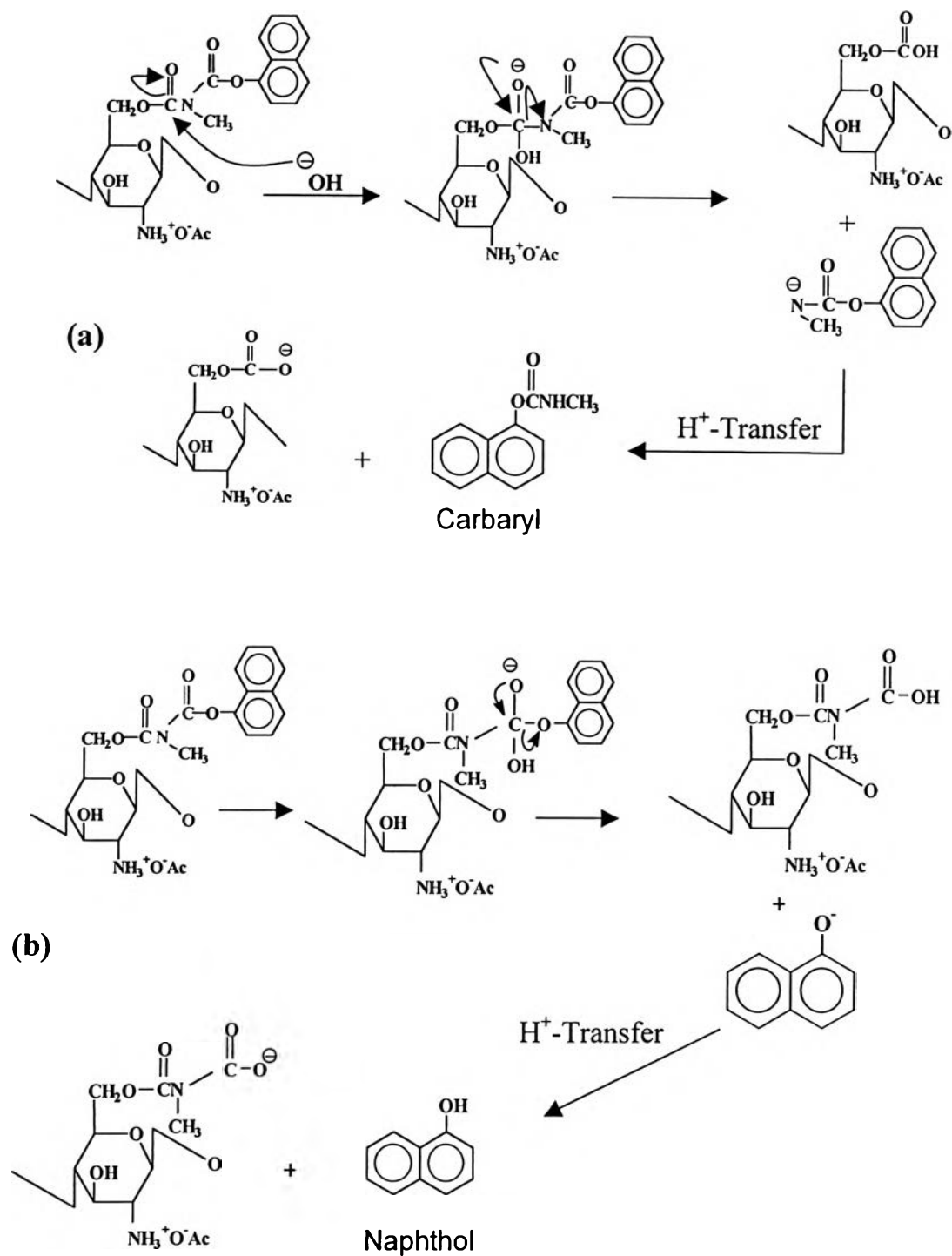
Figure 4.32 Release mechanisms of CA-CDI-CBR via the basic reaction for basic condition at (a) CDI ester position, and (b) carbaryl ester position.
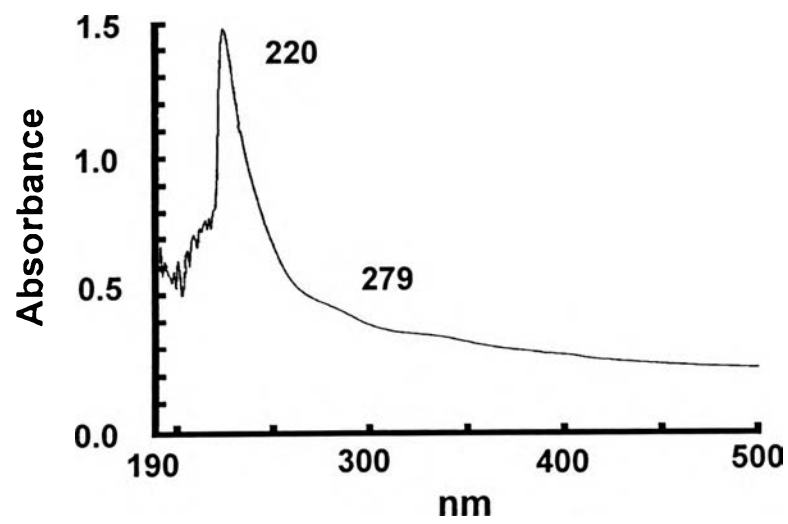
Figure 4.33 UV spectrum of CA-CDI-CBR in 0.01 N NaOH at 60 $^{\circ}$C for 0.5 h.